**The Islamic University Journal (Series of Natural Studies and Engineering)**
Vol.16, No.2, pp 29-40, **2008**, ISSN 1726-6807, http://www.iugaza.edu.ps/ara/research/

# Temperature dependence of the optical nonlinear waveguide sensor on thermal stress effects

**H. J. El-Khozondar[1], R. J. El-Khozondar[2] and M.M.Shabat[3]**
[1]Department of Electrical and computer Engineering, IUG,
P. O. Box 108, Gaza, Palestine; Tel. +970-8-2823311,
Fax: +970-8-2823310, e-mail: hkhozondar@iugaza.edu.ps
[2]Physics Department, Al-Aqsa University, Gaza, Palestinian Authority.
[3]Max Planck Institute for the Physics of Complex Systems, Germany.

**Abstract**: A theoretical approach to study the influence of temperature stress of the thermal sensitivity of the effective refractive index for asymmetrical nonlinear optical waveguides is developed. The structure of the waveguide sensor consists of thin film surrounded by nonlinear cladding and linear substrate. In the proposed waveguide sensor, temperature stress is induced due to the different thermal expansion coefficients of the substrate, core and cladding. Numerical calculation is carried out to draw the thermal sensitivities of effective refractive indices against the core thickness for both transverse electric modes (TE) and transverse magnetic modes (TM). The relation between thermal sensitivities and different temperature stress gradient is derived and plotted. Based on the results, thermal sensitivity of the sensor can be controlled by temperature stresses which can be controlled by carefully picking the materials and loading methods.

**Keywords**: temperature sensitivity, stress, nonlinear waveguide, thermal stress, optical parameters, sensor.

## الاعتماد الحراري لموجة الاستشعار البصرية غير الخطية على آثار الإجهاد الحراري

**ملخص**: :طور نهج النظري لدراسة تأثير درجة الإجهاد الحرارى على الحساسية الحرارية لمعامل الانكسار الفعال لمجس الدليل الموجي البصري غير الخطي وغير المتماثل، ويتكون المجس من شريحة رفيعة محاطة بغطاء غير خطي وركيزة خطية. في مجس الدليل الموجي المقترح، الإجهاد الحراري مستحث بسبب اختلاف معاملات التمدد الحراري للركيزه والشريحة الرقيقة و الغطاء. أجريت حسابات عددية لرسم الحساسية الحرارية لمعامل الإنكسار الفعال مقابل سمك الشريحة الرقيقة **(t)** لكل من الموجات الكهربائية المستعرضة **(TE)** والموجات المغناطيسية المستعرضة **(TM)**. تم اشتقاق ورسم العلاقة بين الحساسية الحرارية لمعامل الإنكسار الفعال وحالات مختلفة للإجهاد الحراري. استنادا إلى النتائج، يمكن التحكم في الحساسيه الحرارية للمجس بواسطة درجة الحراره والتي يمكن التحكم بها بانتقاء المواد المكونة للمجس بعناية وطرق تحميل المواد.

## 1. Introduction

Controlling thermal sensitivity of optical parameters by temperature stress is an important issue in developing optoelectronic devices. The environmental temperature variation induces thermal stresses due to thermal mismatch of different components in photonic devices. The thermal stress causes optical parameters change. This is due to the temperature dependence of the refractive index and optical path length of the waveguide. The variation of the optical parameters, such as wavelength and effective refractive index can be improved so that the resulting change can be used as a measure of the environmental temperature changes. Optical waveguide serves as a transducer that converts perturbations like temperature, stress, strain, rotation or electric and magnetic currents into a corresponding change in the optical radiation [1].

Substantial efforts have been made to enhance the thermal sensitivity of the optical sensor by use of elasto-optic effect. Cohen et al. [2] proposed that stress from differential thermal expansion can be used to control the effects of rising temperature. Oobe et al. [3] used bimetal plate to induce thermal stress to improve the thermal effect of a silica arrayed-waveguide grating. The effective refractive index change under different stress states and the stress effect on the sensitivity of optical waveguides have been considered by Huang [4]. El-Khozondar et al. [5, 6] have investigated the effect of stress on the performance of nonlinear asymmetric waveguide sensor consisting of three layers: nonlinear cladding, linear film and linear substrate. El-Khozondar et al.[7] have studied the stress effect on the nonlinear symmetric waveguide sensor consists of three media: the cladding and substrate media are assumed to be nonlinear and the core medium is considered to be linear.

Temperature sensitivity of the effective refractive index of TE mode of three linear media waveguide has been considered by Huang [8]. The focus of the present study is on the thermal stress effects on the temperature sensitivity of asymmetric nonlinear optical waveguide sensors. Section 2 describes concerning the waveguide sensor configuration. The focus of section 3 is on solving the wave equations and mode equations of the waveguide sensor. In section 4, the attention will be directed towards thermal sensitivity of the effective refractive index. Section 5 is dedicated for Results and discussion, followed by conclusion in section 6.

## 2. Waveguide Arrangement

As shown in Fig. 1, the basic structure of the waveguide in the present analysis consists of three layers: the substrate, the core, and the cladding.

### Temperature dependence of the optical nonlinear waveguide

The core is an infinitely large planar dielectric thin film with thickness of the order of the wavelength. The refractive index of the core is considered higher than the refractive index of the surrounding media. The surrounding media are linear substrate and a nonlinear cladding. The cladding refractive index profile is assumed to have Kerr like intensity dependence expressed as $\varepsilon_{cl}=\varepsilon_0+\alpha\left|E_y\right|^2$, where $\varepsilon_0$ is the linear relative permittivity and $\alpha$ is the nonlinear coefficient [9-11].

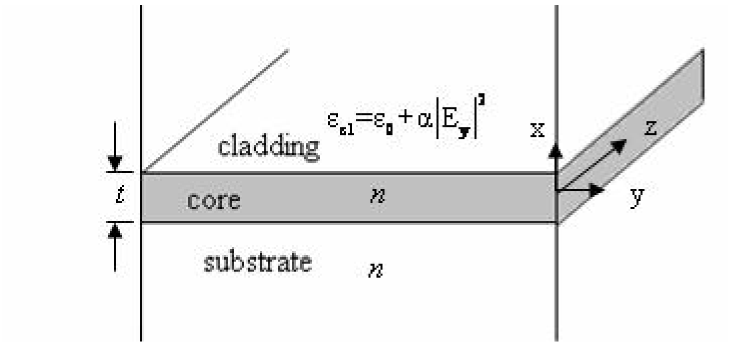


**Fig. 1. Schematic of asymmetric three layer planar waveguide**

The direction of light propagation is parallel to the z axis, confined in the x direction within the central core, and the variation in the y direction is ignored. In this study, the new structure of the waveguide is investigated for both TE and TM fields.

Core is assumed to have a dielectric tensor depend on stress, temperature and strain due to photo-elastic effects [12, 13]. The sheer stresses can be ignored in the z direction because the sensor is considered very long in this direction. Therefore, the relative permittivity tensor of anisotropic material filling the waveguide core is

$$e=\begin{pmatrix} n_{xx}^2 & n_{xy}^2 & 0 \\ n_{xy}^2 & n_{yy}^2 & 0 \\ 0 & 0 & n_{zz}^2 \end{pmatrix}. \quad \textbf{(1)}$$

where $n_{xx}, n_{yy}, n_{zz}$, and $n_{xy}$ are the components of the refractive index, which are functions of x, y, and z.

## 3. The Problem Analysis

The relation between the index and the stress can be expressed by strain-stress relation:

$$\begin{pmatrix} n_{xx} \\ n_{yy} \\ n_{zz} \\ n_{yz} \\ n_{xz} \\ n_{xy} \end{pmatrix} = \begin{pmatrix} n_0 \\ n_0 \\ n_0 \\ 0 \\ 0 \\ 0 \end{pmatrix} - \begin{bmatrix} C_1 & C_2 & C_2 & 0 & 0 & 0 \\ C_2 & C_1 & C_2 & 0 & 0 & 0 \\ C_2 & C_2 & C_1 & 0 & 0 & 0 \\ 0 & 0 & 0 & C_3 & 0 & 0 \\ 0 & 0 & 0 & 0 & C_3 & 0 \\ 0 & 0 & 0 & 0 & 0 & C_3 \end{bmatrix} \begin{pmatrix} \sigma_{xx} \\ \sigma_{yy} \\ \sigma_{zz} \\ \sigma_{yz} \\ \sigma_{xz} \\ \sigma_{xy} \end{pmatrix}, \quad (2)$$

where $C_1 = n_0^3 (p_{11} - 2n\, p_{12}) / (2E)$, $C_2 = n_0^3 [p_{12} - n\,(p_{11} + p_{12})] / (2E)$, and $C_3 = n_0^3 p_{44} / (2G)$ are stress-optic constants. *E*, *G* and *ν* are Young's modulus, shear modulus and Poisson's ratio, respectively. For isotropic crystals, $p_{44} = (p_{11} - p_{12})/2$ and $G = E/2/(1+n)$ [12, 13].

The relation between refractive index and temperature can be expressed by thermo-optic relation:

$$\frac{\partial n}{\partial T} = Bn, \quad (3)$$

where *T* is temperature and *B* is the thermo-optic coefficient, which is usually a function of refractive index, wavelength, and temperature. Combining the effect of stress and temperature on the dielectric film gives the refractive index change as follows,

$$\Delta \begin{pmatrix} n_{xx} \\ n_{yy} \\ n_{zz} \\ n_{yz} \\ n_{xz} \\ n_{xy} \end{pmatrix} = B\Delta T \begin{pmatrix} n_{xx} \\ n_{yy} \\ n_{zz} \\ n_{yz} \\ n_{xz} \\ n_{xy} \end{pmatrix} - \begin{bmatrix} C_1 & C_2 & C_2 & 0 & 0 & 0 \\ C_2 & C_1 & C_2 & 0 & 0 & 0 \\ C_2 & C_2 & C_1 & 0 & 0 & 0 \\ 0 & 0 & 0 & C_3 & 0 & 0 \\ 0 & 0 & 0 & 0 & C_3 & 0 \\ 0 & 0 & 0 & 0 & 0 & C_3 \end{bmatrix} \begin{pmatrix} s_{xx} \\ s_{yy} \\ s_{zz} \\ s_{yz} \\ s_{xz} \\ s_{xy} \end{pmatrix} \quad (4)$$

where $\Delta n = n(T)-n(T_0)$, $\Delta T = T - T_0$; $\sigma_{xx}$, $\sigma_{yy}$, $\sigma_{zz}$, $\sigma_{yz}$, $\sigma_{xz}$, and $\sigma_{xy}$ are stress components. Ignoring the sheer stress effect on optical performance, the stress state in the core can be expressed as

$$s_{xx} = g_x E \Delta g \left(T - T_0\right) + s_{rx}\,, \qquad \textbf{(5)}$$

$$s_{yy} = g_y E \Delta g \left(T - T_0\right) + s_{ry}\,, \qquad \textbf{(6)}$$

$$s_{zz} = g_z E \Delta g \left(T - T_0\right) + s_{rz}\,, \qquad \textbf{(7)}$$

$$s_{yz} = s_{xz} = s_{xy} = 0, \qquad \textbf{(8)}$$

where $\Delta\gamma = \gamma - \gamma_{core}$ is the thermal-expansion coefficient mismatch between the surrounding media and the core medium; $\sigma_{rx}$, $\sigma_{ry}$, and $\sigma_{rz}$ are residual stresses along x, y, z; $g_x$, $g_y$, and $g_z$, are loading parameters which in most cases need to be determined numerically [8].

To simplify the problem and to accentuate the thermal stress effect on the core, the photo-elastic effects are ignored at the surrounding media. The practical waveguide is usually under various stress states due to the thermal mismatch of different layers. Because of the waveguide shape, the stresses are inhomogeneous and anisotropic. The shear stresses are ignored because they have small effect on the optical performance. It is also assumed that the waveguide is under hydrostatic stress state [4, 5]. For example, the loading parameters and residual stresses are independent of x, y, and z. Different loading parameters can bring different thermal stresses in the waveguide.

The field equations for both TE and TM fields are derived below. Applying the appropriate boundary conditions gives the dispersion equations which express the relation between the effective refractive and the thickness of the core for both odd and even modes. TE-mode equations are derived in section 3.1 and TM-mode equations are derived in section 3.2.

### 3.1 TE modes

TE mode is considered when the electric field component in the propagation direction is equal to zero, Ez=0. This will simplify the mode equations in the three layers. The mode equation in the core region [9] , $-t/2 \le x \le t/2$, is

$$\frac{d^2 e_y}{dx^2} + k^2(n^2 - n_e^2)e_y = 0, \qquad \textbf{(9)}$$

where $n$ is the refractive index of the core and $n_e$ is the effective refractive index for TE mode. Solving equation (9) gives

$$e_y = B_e \cos\left(kx\sqrt{n^2 - n_e^2}\right) + C_e \sin\left(kx\sqrt{n^2 - n_e^2}\right). \quad \textbf{(10)}$$

In the substrate region, $x \le -t/2$, the field is

$$e_y = D_e \exp\left(kx\sqrt{n_e^2 - n_s^2}\right), \quad \textbf{(11)}$$

where $n_s$ is the refractive index of the substrate.
The field in the nonlinear cladding, $x \ge t/2$, is

$$e_y = A_e \frac{q_c}{\sqrt{\Lambda}} \operatorname{sech}\left(q_c\left(x - x_0\right)\right), \quad \textbf{(12)}$$

where $q_c = k\sqrt{n_e^2 - e_0}$, $\Lambda = \frac{k^2}{2}a$, and $x_0$ is a constant of integration at maximum power [10, 11]. It has been taken into account that fields approach zero at large values of x for all calculations. The constants $A_e$, $B_e$, $C_e$, and $D_e$ can be determined from the boundary conditions.

At the core-substrate and core-cladding interface, $e_y$ and $h_z \sim de_y/dx$ are continuous at $x = -t/2$ and $x = t/2$ [14]. Applying these boundary conditions produce four homogeneous linear equations. For these equations to have nontrivial solution for the constants, the determinant of the coefficient must be equated to zero [5]. This produces the following dispersion equations

$$\tan p_e = \begin{cases} \left(b_e + \sqrt{b_e^2 + 1}\right); & \text{even modes} \\ \left(b_e - \sqrt{b_e^2 + 1}\right); & \text{odd modes} \end{cases} \quad \textbf{(13)}$$

where $p_e = \frac{kt}{2}\sqrt{n^2 - n_e^2}$, $b_e = \tan\left(k_{e1} - k_{e2}\right)$, $\tan\left(k_{e1}\right) = \sqrt{\frac{n_e^2 - n_s^2}{n^2 - n_e^2}}$,
$\tan\left(k_{e2}\right) = \frac{k\sqrt{n^2 - n_e^2}}{h}$, and $h = q_c \tanh\left(q_c\left(\frac{t}{2} - x_0\right)\right)$.

## 3.2. TM modes

TM mode is considered when the magnetic field component in the direction of propagation is equal to zero, $H_z$=0. The mode equation [15] of the core, $-t/2 \le x \le t/2$, is

$$\frac{d^2 h_y}{dx^2} + k^2 (n^2 - n_h^2) h_y = 0, \qquad \textbf{(14)}$$

and its solution is

$$h_y = B_h \cos\left(kx\sqrt{n^2 - n_h^2}\right) + C_h \sin\left(kx\sqrt{n^2 - n_h^2}\right), \qquad \textbf{(15)}$$

where $n_h$ is the effective refractive index for TM mode.
In the linear substrate, region, $x \le -t/2$, the field form is

$$h_y = D_h \exp\left(kx\sqrt{n_h^2 - n_s^2}\right). \qquad \textbf{(16)}$$

In the nonlinear cladding region, $x \ge t/2$, the field is expressed as

$$h_y = A_h \frac{q_c}{\sqrt{\Lambda}} \operatorname{sech}\left(q_c\left(x - x_0\right)\right), \qquad \textbf{(17)}$$

where $q_c$, $\Lambda$ and $x_0$ are defined earlier. The boundary conditions of zero fields at large values of x are considered in all calculations. $A_h$, $B_h$, $C_h$, and $D_h$ are constants. At the interface between core and cladding, the boundary conditions are the continuity of $h_y$ and $e_z \sim n^{-2}\, dh_y/dx$ across the boundary [14]. The same procedure is used for TE mode gives the following dispersion equations

$$\tan p_h = \begin{cases} \left(b_h + \sqrt{b_h^2 + 1}\right); & \text{even modes} \\ \left(b_h - \sqrt{b_h^2 + 1}\right); & \text{odd modes} \end{cases} \qquad \textbf{(18)}$$

where

$$p_h = \frac{kt}{2}\sqrt{n^2 - n_h^2}\,, b_h = \tan\left(k_{h1} - k_{h2}\right),\ \tan\left(k_{h1}\right) = \frac{n^2}{n_c^2 n_s^2}\sqrt{\frac{n_h^2 - n_s^2}{n^2 - n_h^2}},$$

$$\tan\left(k_{h2}\right) = \frac{k\sqrt{n^2 - n_h^2}}{n^2 h}, \textbf{ and } h = q_c \tanh\left(q_c\left(\frac{t}{2} - x_0\right)\right).$$

## 4. Thermal Sensitivity of the Effective Refractive Index

Thermal sensitivity of effective refractive index of nonlinear optical waveguides under thermal stress is defined as the absolute value of the rate of change of effective refractive index with respect to temperature, $|dn_i/dT|$. The thermal sensitivity is calculated by Differentiating equation (13) for TE and equation (18) for TM with respect to temperature, T. The thermal sensitivity of effective refractive index of the even and odd modes has identical shape as

$$\sec^2(p_i)\frac{dp_i}{dT} = \frac{b_i + \sqrt{b_i^2+1}}{\sqrt{b_i^2+1}}\frac{d\,b_i}{dT}. \qquad \textbf{(19)}$$

where *i* denotes *e* for TE and *h* for TM. Change of the core refractive index with respect to temperature, $dn/dT$ can be found from equation (4).

## 5. Numerical Results

In Fig. 2 , the temperature sensitivity, $dn_e/dT$, is plotted as a function of the core thickness for the zero mode of the TE fields. The temperature sensitivity varies with the core thickness. As the core size increases, the temperature sensitivity increases until certain cutoff (t=1µm), then it drops. The temperature sensitivity for the zero mode of the TM field, $dn_h/dT$, as a function of core thickness is displayed in Fig. 3. The temperature sensitivity of the TM mode increases with increasing core thickness. It is also noticeable that there is a dip around 5.5 µm at which the sensitivity deceases, then increases again. The temperature sensitivity of the effective refractive index of the zero mode for both TE and TM are plotted as a function of different thermal stress gradients in Fig. 4 and Fig. 5 respectively for different core thicknesses. Fig. 4 and Fig. 5 demonstrate that the higher the core thickness the higher the temperature sensitivity of the effective index for all thermal stress gradient values. All curves intersect at thermal stress gradient value equal to 3 $^{o}C^{-1}$. In all the calculations, the values of the optical parameters are: $n_0$=3.5, $n_1$=3.4, $\varepsilon_0$=2.7, $\alpha=10^{-9}$ $m^2/W$, $\lambda$=0.83µm, and $C_1/C_2$=0.1.

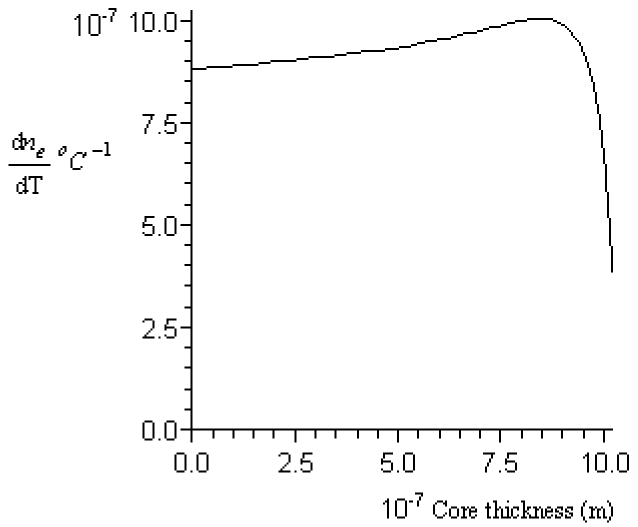


**Fig. 2. Temperature sensitivity of effective refractive index of the TE zero mode (m=0) as a function of core thickness.**

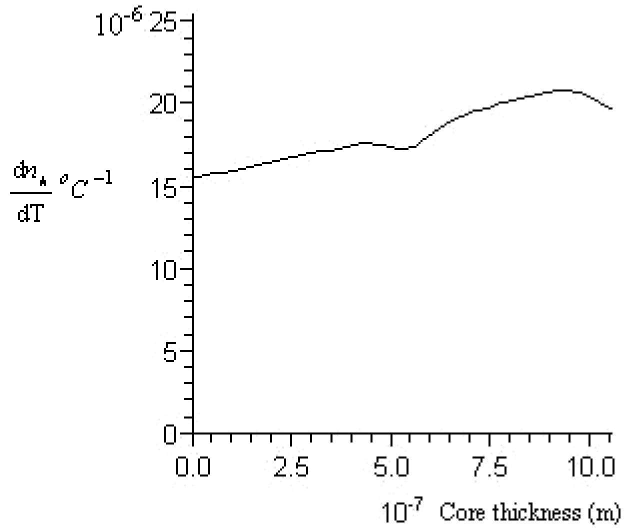


**Fig. 3. Temperature sensitivity of effective refractive index of the TM zero mode (m=0) as a function of core thickness.**

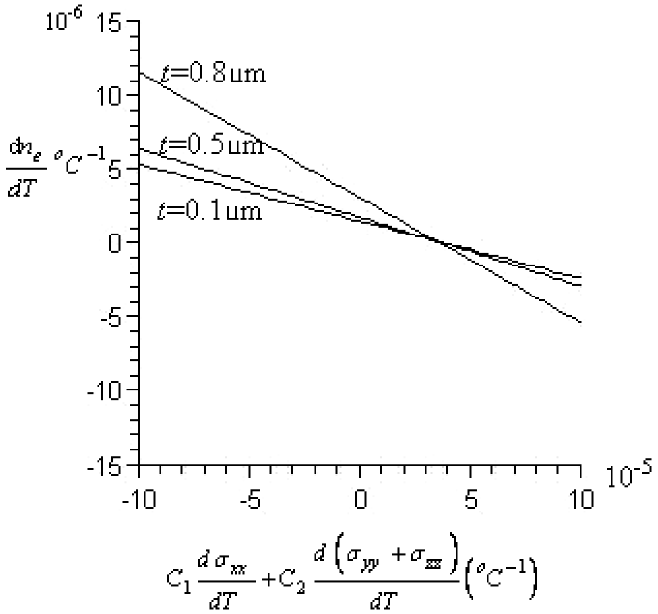


**Fig. 4. Temperature sensitivity of the effective refractive index of the TE fundamental mode (m=0) for a planar waveguide sensor versus different thermal-stress gradients for various values of core thickness (*t*).**

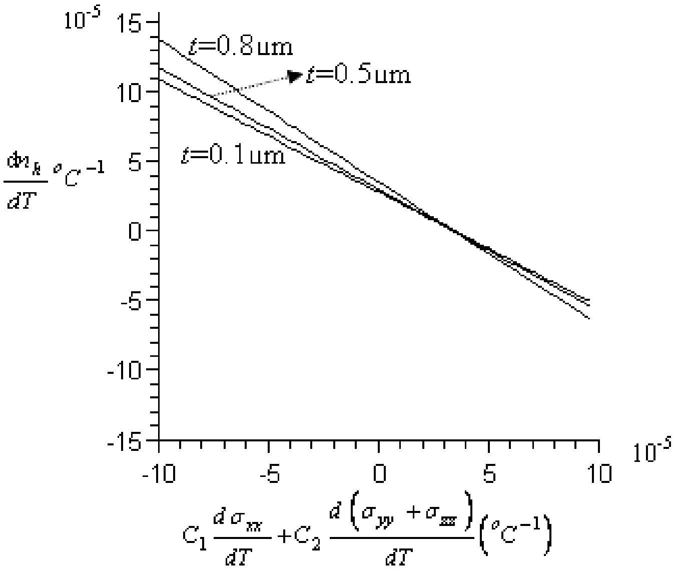


**Fig. 5. Temperature sensitivity of the effective refractive index of the TM fundamental mode (m=0) for a planar waveguide sensor versus different thermal-stress gradients for various values of core thickness (*t*).**

## 6. Conclusion

In the present paper, analytical solutions are developed to estimate the effects of thermal stress on the temperature sensitivity of optical nonlinear waveguide sensors. It is found that thermal sensitivity of nonlinear waveguide sensors can be controlled by thermal stresses. Thermal stress in the waveguide can be controlled by carefully picking the materials and loading methods. Consequently, the temperature sensitivities of the effective refractive index can be tuned cautiously. Therefore, introducing suitable thermal stresses, elevated temperature sensitivity will cause a wider tuning range in tunable filters and lasers. The approximate solutions developed in this article can be conveniently used to guide the preliminary design to consider temperature stress effects to enhance the performance of the waveguide sensors by enhancing their performance through consideration of temperature stress effect.

## REFERENCES

[1] Ghatak, A. and Thyagarajan, K., *Introduction to Fiber Optics*. UK: Cambridge University Press (1998).

[2] Cohen, D. A., Heimbuch, M. E., and Coldren, L. A., "Reduced temperature sensitivity of the wavelength of a diode laser in a stress-engineered hydrostatic package," *Appl. Phys. Lett.* **69 (4)**, 455-457 (1996).

[3] Ooba, N., Hibino, Y., Inoue, Y., and Sugita, A., " Athermal silica-based arrayed-waveguide grating multiplexer using bimetal plate temperature compensator," *Electron. Lett.* **36**, 1800-1801 (2000).

[4] Huang, M., "Stress effect on performance of optical waveguides", *International Journal of Solids and Structures* **40**, pp 1615-1632 (2003).

[5] El-Khozondar, H., El-Khozondar, R., Shabat, M., Kock, A., "Stress effect on optical nonlinear waveguide sensor", *J. Optical communication*, **28 (3)** in press.

[6] El-Khozondar, H. J. "Hydrostatic Stress Effect on the Optical Performance and the Stress Sensitivity of Optical Nonlinear Waveguide", *Annjah Journal for research (natural science),* accepted (2007)

[7] El-Khozondar, H., Shabat, M., Abu Tair, G., and Abadla, M., "Thermal-stress effects on nonlinear thin film Waveguide Sensors," *Journal of Physics & Chemistry of Solid State* **8 (2)** 260-264 (2007).

[8] Huang, M., Yan, X., “Thermal-stress effect on the temperature sensitivity of optical waveguides”, *J. Opt. Soc. Am. B* **20 (6)**, 1615-1632 (2003).

[9] Boardman A., and Egan, P., “Optically nonlinear waves in thin films”, *IEEE of quantum electronics*, **QE. 22 (2)**, 319-324 (1986).

[10] Khozondar, H., Saifi, R., Shabat, M. M., “Nonlinear surface wave guided by a single periodic medium”, *Laser Physics* **14 (12)**, 1539-1543 (2004).

[11] Stegeman, G., Seaton, C. T., Ariyasu, J., Wallis, R., Maradudin, A., “Nonlinear electromagnetic waves guided by a single interface”, *J. Appl. Phys.* **58 (7)**, 2453-2459 (1985).

[12] Xu, J., Stroud, R., *Acousto-optic Devices: Principles, Design, and Applications*. New York: John Wiley and Sons (1992).

[13] Sapriel, J., *Acosto-optics*. New York: John Wiley and Sons (1979).

[14] Boyd, J., Photonic integrated circuits. In: R. G. Hunsperger, *Photonic Devices and Systems*, New York: Marcel Dekker (1994).